Sādhanā, Vol. 17, Parts 3 & 4, September 1992, pp. 391–409. © Printed in India.

Integrated optics – technology and applications

A SELVARAJAN

Department of Electrical Communication Engineering, Indian Institute of Science, Bangalore 560012, India

Abstract. The emergence of optoelectronics and photonics as viable alternatives to electronics in many key areas of engineering relevance is indeed significant. This paper presents a tutorial review of integrated optics – a technologically important development in photonics. Materials, processes, device technology and applications are highlighted.

Keywords. Integrated optics; photonic circuits; technology; applications.

1. Introduction

With the advent of lasers, semiconductor optoelectronic sources and detectors, and optical fibres, many new applications using photonics have emerged. The foremost among them is optical fibre communication. Such fibre systems are now deployed not only in the long-haul corridor applications but also in metropolitan trunking networks and local subscriber loops. However much progress remains to be achieved before the full potential of optical fibre transmission, in particular, and photonics in other areas of applications, in general, is exploited. It is expected that integrated optics and integrated optoelectronics will play key roles in attaining the long-term objectives of photonics.

Electron devices have evolved in stages from electron tubes to transistors to integrated circuits (ICs). Currently in microelectronics very small device dimensions and very large package densities are commonly realized. A similar advance is essential in photonics if optical systems are to be competitive and compact as compared to electronic systems. In other words miniaturized optical components integrated on a 'Chip' will greatly enhance the application potential of photonics. The term Integrated Optics (IO) was proposed about 22 years ago by Miller (1969). It was then visualized that thin films and microfabrication technology could be suitably adopted to realize optical counterparts of integrated electronics for generation, modulation, switching, multiplexing, processing and such other optical functions in IO form. However, there were limitations in the practical realization of optical ICs due to the fact that the theory and technology were relatively new and that microfabrication methods needed further research and development. Fortunately, the hesitant start soon gathered rapid momentum due to practical necessities arising out of quick deployment of optical communication and sensing systems. There are strong indications that processing and computing systems will soon follow suit. It is in this context that the technology and application of integrated optics is to be viewed as adding a new and exciting dimension to photonics. The theory of waveguides and devices for IO is well known (Kogelnik

1975; Ghatak & Thyagarajan 1989). In this paper the emphasis is on the technology and applications of IO.

2. Materials for integrated optics

The requirements of materials for IO are essentially the same as those of optics and optoelectronics in general. Since thin film techniques play the main role, materials for IO should be amenable for thin film technology. Optically transparent materials with ability to form homogeneous crystalline structures in micrometer thickness are best suited for IO since functional integration will then be broadbased. The role of amorphous material is limited to some passive circuits. Broadly, there is a need for appropriate substrate materials on the one hand and materials for thin guiding layers on the other hand. Most often, though, the guiding region is created in the substrate material itself by appropriate doping, diffusion and such other means.

Glasses are well known in optics. These are composed of SiO_2 plus small proportions of other oxides – B_2O_3, Na_2O, CaO etc. A simple fabrication process – ion exchange in glass – has already been well developed for IO. Another advantage of glass-based IO is that it is compatible with optical fibres in terms of composition and refractive index and therefore can easily be interconnected. The main drawback is that only certain passive functions can be realized since glasses in general do not exhibit externally controllable properties such as electrooptic (EO), acoustooptic (AO) and nonlinear optic effects. Nevertheless, IO devices on glass are likely to be popular due to low cost and ease of fabrication.

Dielectric crystals are better than glasses because pronounced EO, AO and nonlinear effects are known at least in certain crystals such as $LiNbO_3$, KDP, KTP, BSO etc. The main difficulty is that the growth of such crystals in large sizes is cumbersome and costly. Lithium niobate ($LiNbO_3$) has proved to be an outstanding candidate for IO with nearly all application oriented devices and circuits reported till now being in $LiNbO_3$. However since sources and detectors cannot be readily realized with $LiNbO_3$, the integration is only partial or hybrid.

Well known semiconducting materials such as silicon and gallium arsenide extensively used in electronics are another class of materials under investigation for IO. The main advantage in using these materials is that optical sources and detectors can be directly built in the same substrate along with other optical circuits. Also, since a certain amount of electronic circuits like drivers for sources and amplifiers for detectors are also needed, these can also be integrated along with optical circuits in the same material. There is also the added advantage that processing and handling of semiconductor materials such as Si and GaAs are well known due to their popularity in the electronics industry.

Polymers are another class of materials which are likely to offer low cost solutions in many IO applications. Recently some polymers which exhibit large nonlinear coefficients have been studied (Van Tomme *et al* 1991). These are attractive in terms of achieving efficient second harmonic generation, bistability, switching and other forms of photonic signal handling. Polymers have the disadvantage in that they show large temperature dependence and poor shelf life. Also some of the new polymers are not commercial. It is also difficult to achieve complete integration as is possible with semiconductors mentioned earlier. Polyvinylidine fluoride (PVF_2) is one of the promising polymer materials for IO. It shows piezoelectric, pyroelectric, dielectric and

nonlinear properties in good measure. Polystyrene, polyurethene, polymethyl methacrylate, polyimide and many other polymers have been investigated for their role in IO.

3. Process technology

There are several ways by which waveguides and devices in IO form can be realized. The type of material chosen more or less decides the process technology to be employed. In the case of glass, wet and dry ion exchange techniques (Ramaswamy & Srivastava 1988) are commonly used for fabricating mostly passive IO components such as splitter/combiners. Polymer waveguides on glass or other substrates on the other hand are formed by spin or dip coating. While this process is simple, precise thickness and uniformity control are difficult. Plasma polymerization and Langmuir–Blodgett method of formation are other techniques used in the case of polymers. The most popular material for IO, $LiNbO_3$, can be processed either using metal in-diffusion – usually titanium (Burns *et al* 1979) or by proton exchange in weak acids (Loni *et al* 1989). Epitaxial methods (LPE, MBE, MOCVD) are appropriate for the growth of crystalline layers and quantum well structures in semiconductors (Deri & Kapon 1991). Amorphous layers on silicon are also useful in certain passive component development such as grating and channel waveguides for WDM and LAN applications (Takato *et al* 1988; Shani *et al* 1991). Most of these processes are well understood and additional information can be obtained from the literature cited above.

There are certain prefabrication procedures which are to be carefully followed before an actual waveguide/device process is initiated. It is absolutely essential if low loss IO components and systems are to be achieved. Substrate preparation in terms of polishing and cleaning are the critical prefabrication processes. Dust-free environment, temperature and humidity control and prevention of inadvertent contamination are additional precautions to be followed.

3.1 *Analysis on dry exchange process in glass*

The major theoretical work in this area has been to calculate the refractive index profile that will be obtained after processing. A diffusion equation is generally the starting point for all such work.

In the one-dimensional accurate analysis of the process, Honkanen & Tervonen (1988) found that in order to get a desired refractive index profile the evolution of the silver ion concentration profile in different conditions has to be known, as the refractive index increment is almost linearly related to the concentration of silver ions. The total amount of silver ions in glass can easily and accurately be controlled by the ion exchange time and the current density, since the only reaction introducing the silver ions into the glass is the electrochemical anode reaction in which the silver oxidizes. The time needed to drive whole film into the glass is,

$$t = d\rho F/(M_{Ag} I),$$

where d = film thickness, ρ = density of silver, F = Faraday constant, M_{Ag} = molecular weight of Ag, and I = ion current density.

During the field assisted ion exchanges the flux density of silver and sodium ion

in one dimension is,

$$j_{Ag} = \left[D_{Ag}\left(\frac{eEC_{Ag}}{KT}\right) - D_{Ag}\left(\frac{\partial C_{Ag}}{\partial x}\right)\right],$$

$$j_{Na} = \left[D_{Na}\left(\frac{eEC_{Na}}{KT}\right) - D_{Na}\left(\frac{\partial C_{Na}}{\partial x}\right)\right].$$

Here it is assumed that the self diffusing coefficient $D_i = M_i K_i T$ of the two ions are constant functions of position x and concentration C_i. E varies with x and t because of the different mobilities of the two ions. The local electrical neutrality requires that,

$$C_{Ag} + C_{Na} = C_0 \quad \text{(constant)},$$

$$j_{Ag} + j_{Na} = j_0 \quad \text{(constant)}.$$

where, C_0 = initial sodium ion concentration, and $j_0 = I/F$.

From these the electric field can be written as,

$$E = \left(\frac{kT}{e}\right)\frac{[Mj_0 + D_{Ag}(M-1)(\partial C_{Ag}/\partial x)]}{D_{Ag}[C_0 + (M-1)C_{Ag}]},$$

where $M = M_{Ag}/M_{Na}$ = mobility ratio of the ions.

Using the continuity condition for silver ions, i.e.

$$\partial C_{Ag}/\partial t = -\partial j_{Ag}/\partial x,$$

we get a second-order differential equation for the ion exchange process:

$$\frac{\partial C_{Ag}}{\partial t} + \frac{Mj_0 C_0}{[C_0 + (M-1)C_{Ag}]^2}\frac{\partial C_{Ag}}{\partial x} = D_{Ag}\frac{\delta}{\partial x}\frac{C_0(\partial C_{Ag}/\partial x)}{[C_0 + (M-1)C_{Ag}]}.$$

The above equation can be solved analytically only if the electric field gradient caused by the different mobilities of the two ions is neglected or if the exchange time is long enough and a profile with a stationary shape can be assumed. In commonly used sodium glasses, $M_{Ag}/M_{Na} \approx 0{\cdot}1$ and in the case of silver film ion sources, the $Ag^+ \leftrightarrow Na^+$ exchange is complete. Therefore the electric field gradient has to be taken into account. The solution of the stationary state including the effect of the mobility difference is,

$$\frac{C_{Ag}}{C_0} = \left[1 + \exp\frac{j_0(1-M)}{D_{Ag}C_0}\left(x - \frac{j_0 t}{C_0}\right)\right]^{-1}.$$

Knowing x and t, the relative silver ion concentration C_{Ag}/C_0 can be calculated and then n can be determined. Hence the RI profiles can be plotted as a function of depth and time.

3.2 *Proton exchange in $LiNbO_3$*

The proton exchange process first proposed in 1982 has been developed into a mature technology for fabricating IO devices on $LiNbO_3$. The ease of fabrication at low temperature involving immersion of the wafer in molten benzoic acid (C_6H_5COOH)

for periods of a few minutes to produce single mode waveguides or longer times for multimode waveguides has been the chief attraction in this case. A large n_e index change in the waveguide region with a step index profile and a high resistance to optical damage are other desirable features of proton exchange (PE). In contrast, the other well known process, namely Ti indiffusion, is a high temperature process, results in graded index profiles and is prone to optical damage. Proton exchange process yields a reduced n_0 and therefore is useful in the operation of leaky wave polarization devices.

PE in $LiNbO_3$ involves the replacement of Li ions by equal numbers of protons when the substrate is immersed in a proton source such as molten acid. The physical process can be depicted as below.

$$C_6H_5COOH \leftrightarrow C_6H_5COO^- + H^+,$$

$$LiNbO_3 + xH^+ \leftrightarrow Li_{1-x}H_xNbO_3 + xLi^+,$$

$$LiNbO_3 + C_6H_5COOH \leftrightarrow Li_{1-x}H_xNbO_3 + C_6H_5COOLi_x.$$

The PE process is very successful with X- and Z-cut $LiNbO_3$ crystals while in the case of Y-cut (often used in surface acoustic wave applications) there results a severe surface damage. It has been shown that the control of melt composition can prevent surface damage.

Another method involves the use of previously Ti-diffused $LiNbO_3$ for PE. This is called the TIPE process. Proton exchanged layers of $LiNbO_3$ have been characterized using various techniques such as X-ray diffraction, Rutherford back-scattering, electron microscopy, secondary ion mass spectroscopy, IR absorption and the usual prism coupling scheme for mode line spectroscopy. The objective of all these measurements is essentially to obtain an indepth understanding of structural and chemical changes that take place and to arrive at means to combat undesirable effects responsible for poor performance.

3.3 *IO devices by silica based on silicon*

Silicon technology is well established due to its predominant role in electronics. If low loss waveguides and devices can be built in silicon, existing technology can be profitably used. It is in this context silica-based waveguides have been studied by some groups. One main advantage of this approach – as also in the case of glass – is the compatibility with fibre optic systems resulting in efficient power transfer from IO to fibre systems.

Pure and doped SiO_2 and Si_3N_4 core and buffer layers are formed on a silicon substrate by flame hydrolysis, low pressure chemical vapour deposition and other similar means. Multiplexing and demultiplexing devices, splitters etc. for communications, sensing and signal processing are some of the practical uses of silica in silicon-based integrated optics reported in the recent literature (see Brabander *et al* 1991).

4. IO devices

Photonic circuits for various applications can be implemented if the required functional devices in IO form are well understood. Guided wave devices and

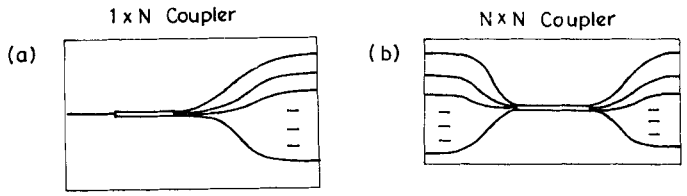

Figure 1. (a) $1 \times N$ and (b) $N \times N$ star couplers.

components can be broadly grouped into passive and active devices. A passive device is one in which there is no control phenomena such as electro- or acoustooptic control and there is no scope for generation, amplification or switching of light. Optical couplers, beam dividers, lenses, polarizers etc. belong to this category. In contrast, active devices which are the basic functional devices such as modulator, switch, amplifier etc., need dielectric single crystals or semiconducting materials. Besides the well developed electro, acousto, magneto and thermal effect devices, currently control of light by light through nonlinear effects is gaining importance.

4.1 *Passive star coupler*

Optical star coupler is a device which distributes power equally among all of the output ports from any of the input ports (figure 1). It is a key device for use in local area network systems as well as in the newer 'broadcast and select' multiwavelength photonic networks. In typical LAN applications the coupler can be a multimode device while in high speed networks it should be a single mode device. Multimode devices by ion exchange in glass and polymers have been reported earlier. Recently a 1×128 coupler on silicon using single mode WG was reported (Takahashi *et al* 1991). A detailed design procedure using ray tracing and some analytical results have been reported by us (Selvarajan 1986). In this design of a multimode 4×4 star coupler it was shown that for a horn angle of 6° and a mixing length of 6·8 mm, equal distribution of light to all ports occurs, and that the fractional loss of rays increases with increasing horn angle.

4.2 *IO polarizers*

Accurate control of polarisation is essential in a number of optical circuits like switching networks, high dynamic range intensity modulators and fibre gyro circuits. Otherwise, power in the unwanted mode results in increased crosstalk in switching networks, decreased dynamic range in intensity modulators and bias drift in fibre gyro circuits. Polarization maintenance, discrimination and control are essential requirements in integrated optical guided wave circuitry for effective system performance measures.

A variety of techniques have been reported in the recent past to cater to the needs of polarization control in IO form. These methods can be classed as:

1. the metal overlay technique;
2. the anisotropic overlay technique;
3. the dielectric/metal resonant structure;
4. a tuned directional coupler;
5. a short section of proton exchanged waveguide.

In a typical metal clad waveguide, for example, aluminium overlay of a few mm length, the TM modes are at least ten times as lossy as their TE counterparts. This phenomenon can be readily exploited to construct optical integrated polarizers.

From the experimental and analytical studies made by Takano & Hamasaki (1972) on metal clad dielectric slab waveguides it was readily concluded that the metal clads of dielectric slab waveguides perform discrimination of modes of different polarizations. The physical origin of the loss was attributed to the absorption of the tail of the field profile that extends into the lossy metal. The polarization attenuation ratio varies among metals and seems to be highest for aluminium for which it reaches 11·5 dB/cm. The limitation of this method is that the metal cladding attenuates both the modes resulting in a high excess loss. Thus it may be difficult to achieve a significant extinction ratio without introducing a significant loss in the transmitted light.

In the anisotropic overlay/cladding technique the composite structure acts like a leaky waveguide for one type of polarization while guiding the other type of polarization without significant loss. For standard crystal orientation, the TE and TM waves in $LiNbO_3$ see either the ordinary or the extraordinary index. Two methods are available for utilising $LiNbO_3$ to construct TE and TM polarizers (see figure 2). The first is to employ a birefringent superstrate. Depending on the orientation of the waveguide substrate used the superstrate can be oriented such that either a TE pass or a TM pass polarization is obtained. In the case of a Z-cut $LiNbO_3$ substrate TE and TM modes see the ordinary and extraordinary indices respectively.

The second method is compatible with planar thin film technology and is more appropriate in IO. Here a film of an amorphous dielectric whose RI is $n_e < n_f < n_0$ is deposited upon the surface of the waveguide. Thus TE pass polarizers are formed on either X- or Y-cut substrates.

A proton-exchanged polarizer consists of Ti-diffused channel waveguide with short discontinuities that are filled with proton-exchanged waveguides as shown in figure 2c. In the proton-exchanged waveguides, the change in extraordinary index n_e is positive while n_0 is negative. Thus the extraordinary ray is guided along the entire length of the structure and thus experiences minimal insertion loss. The ordinary mode on the other hand is not guided in the proton-exchanged region and radiated into the substrate.

Of all these techniques, the dielectric/metal resonant structure and the proton

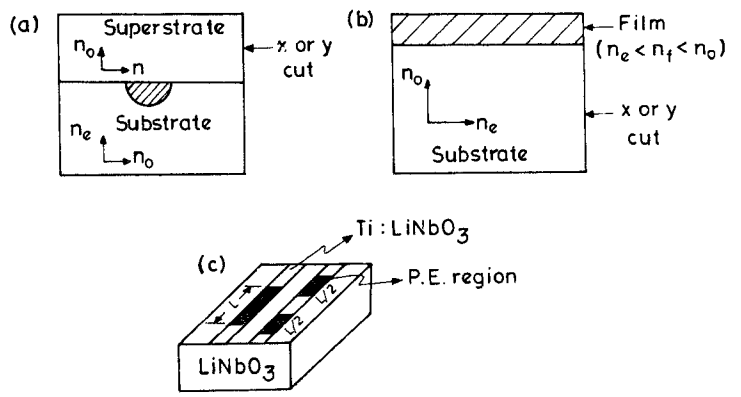

Figure 2. Integrated optic polarizers using (**a**) birefringent superstrate, (**b**) thin film and (**c**) proton exchange.

exchanged polarizer are the most promising since they are monolithic, short (< 4 mm) and offer high polarization extinction (> 40 dB) with low insertion loss (< 1 dB). The proton-exchange technique has the added advantages that it is adaptable to all crystal cuts and is relatively insensitive to changes in the operating wavelength and the fabrication parameters (Findalky & Chen 1984).

4.3 *Thin film lenses*

Several generic types of integrated optical lenses have been demonstrated using a variety of principles of operation. The three major categories are shown in figure 3. These lenses are required in optical signal processing and computing circuits such as the RF spectrum analyser, matrix multiplier etc.

The Luneberg lens is circular and symmetric, and employs a radial refractive index profile that increases towards the centre. This profile can be achieved either by modifying the WG, or by depositing an overlay film on to the WG, using masking techniques to achieve the required thickness profile and hence perturb the effective index of the guided mode. The focusing action, which is due to the increased optical path length in the modified region, is similar in principle to that of a bulk lens.

Geodesic lenses are formed by the single point diamond turning of a circularly symmetrical depression in the substrate prior to WG formation, and focusing occurs according to Fermat's principle.

Grating lenses (Bragg and Fresnel) use the diffraction of light by the grating to give the focusing effect. Other possible planar lens configurations are microlens arrays, multielement thin lenses and curved parabolic edge reflectors.

A common characteristic of all the lenses mentioned above is the difficulty in obtaining a combination of all desirable lens characteristics. The microlens described below can facilitate the making of complex lenses such as microlens arrays and composite lenses.

Let us assume an arbitrary convex boundary $C(x, y)$ as shown in figure 4. The system is fabricated in such a way that the effective extraordinary index of refraction (n_e) in region II is higher than that of the region I (Ti).

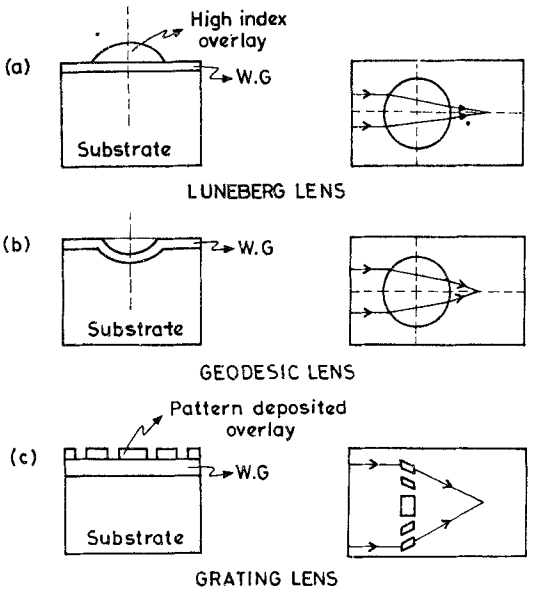

Figure 3. Different integrated optic lenses: (**a**) Luneberg, (**b**) geodesic and (**c**) grating types.

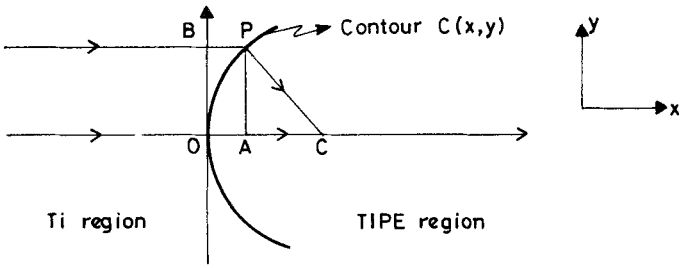

Figure 4. Design of a TIPE IO lens.

The contour $C(x, y)$ can be determined as follows by applying Fermat's principle.

$$n_e \cdot \overline{BP} + n'_e \overline{PC} - n'_e \overline{OC} = 0.$$

Setting $\overline{BP} = x$, $\overline{OB} = y$ and $\overline{OC} = F$, we have

$$n_e \cdot x + n'_e[(F-x)^2 + y^2]^{1/2} - Fn'_e = 0$$

or

$$n_e x + n'_e[F^2 + x^2 - 2Fx + y^2]^{1/2} - Fn'_e = 0$$

or

$$n_e^2[F^2 + x^2 - 2Fx + y^2] = (Fn'_e - n_e x)^2,$$

where F = focal length and n_e and n'_e are RIs in the two regions.

The above equation can be rearranged to give an equation of ellipse as below.

$$\left[x - \frac{F}{(1+(n_e/n'_e))}\right]^2 \Big/ \left[\frac{F}{(1+(n_e/n'_e))}\right]^2 + y^2 \Big/ \left[\frac{F[1-(n_e/n'_e)^2]^{1/2}}{(1+(n_e/n'_e))}\right]^2 = 1.$$

On appropriate substitution of the values of n_e, n'_e and F the above equation assumes a simple form.

This design can be illustrated further with the following practical example.

In the case of titanium indiffused proton-exchanged (TIPE) $LiNbO_3$ waveguide lenses

$$n_e \approx 2{\cdot}211 \text{ and } n'_e \approx 2{\cdot}32.$$

Hence we get

$$\frac{(x - 0{\cdot}512F)^2}{(0{\cdot}512F)^2} + \frac{y^2}{(0{\cdot}156F)^2} = 1.$$

So the contour of the boundary $C(x, y)$ is an ellipse. The aperture of the lens is equal to twice that of the minor axis, i.e.,

$$A = 2 \times 0{\cdot}156F = 0{\cdot}312F.$$

Hence, for a given focal length one can determine the contour and aperture of the lens. The spot size at the focus for an ideal lens is given by $F\lambda/A$.

In actual fabrication of the single mode microlenses, Zang & Tsai (1985) made use of the well established TI process first to form a planar WG in Y-cut $LiNbO_3$. Subsequently, a masking material such as Si_3N_4 with a designed lens contour was deposited on the TI WG. The sample was then immersed in molten C_6H_5COOH at

230°C for 6 h. Thus the lens region alone undergoes PE also. This TIPE region of appropriate contour functions as a planar waveguide lens.

4.4 *Waveguide modulators*

High speed modulators and beam deflectors that make use of electrooptic or acoustooptic interactions in optical waveguides have been in use for the last several years. Of these, waveguide electrooptic modulators are found to be the most useful for efficient, high speed modulation and switching (see Alferness 1982). The performance of such devices are often described in terms of the required electrical modulating power to produce a given degree of modulation over a specified bandwidth. The performance depends on the operating wavelength, the properties (in particular the EO coefficient) of the waveguide material and the device geometry. It has been shown that IO modulators are much more efficient than their bulk counterparts due to a substantial improvement in the geometrical factor (in terms of small cross-section and light confinement over long lengths). As a result the modulating power per bandwidth improves from mW/MHz to mW/GHz. However, the improved efficiency can be important in practice only if wideband modulation is considered. To increase the frequency response well into the microwave region, travelling wave electrode geometry is to be adopted. The factors engaging the attention of researchers involved with the design of high speed modulators were: increasing the bandwidth, decreasing the drive power, reducing the electrode conductor loss and overcoming impedance mismatch. Thus there evolved a suitable electrode geometry from lumped to travelling wave to phase reversal types to achieve high speed modulation simultaneously with low drive power.

There has been considerable research activity in the analysis of direct microwave modulation of optical signals using integrated electrooptic modulators. Static techniques such as conformal mapping, method of images and method of lines have been known. Recently, a finite difference method (FDM) has been developed by the author's group (see Satyanarayana *et al* 1992). Analytical calculations of IO modulators are complicated because the index profiles are not only a function of the surface coordinates but also a function of depth, thus making it a three-dimensional problem. One way to handle this problem is to use the beam propagation method (BPM) developed by us (Shivakumar *et al* 1990).

4.4a *Phase modulator.* An integrated optic phase modulator is shown in figure 5. Application of a voltage (V) causes a small change in refractive index given by

$$\Delta n = (n^3 r/2)/(V/d),$$

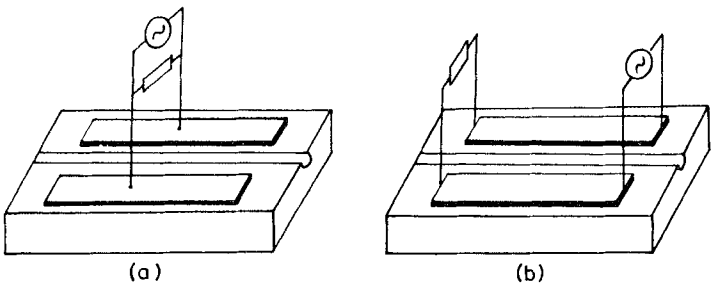

Figure 5. Electrooptic phase modulators (**a**) lumped and (**b**) travelling wave types.

where n is the appropriate index in the absence of voltage, r is the proper electrooptic coefficient and d is the separation between electrodes. Consequent to the change in index, a phase change given by

$$\Delta\phi = (2\pi/\lambda)\Delta n \cdot L,$$

also occurs at the output of the waveguide, where L is the length of the electrode and λ is the wavelength.

Combining the two equations and rewriting, taking modulation to be π, we get

$$VL = (\lambda d)/(n^3 r\Gamma),$$

where Γ is an overlap factor between the electric field and the optical mode field. Optimization of Γ forms an important aspect of modulator design.

In the case of a phase modulator many electrode geometries are possible. The lumped electrode phase modulator has been shown to give a 3 dB bandwidth of

$$\Delta f_{3\text{dB}} = 1/(\pi \text{Rc}).$$

Modulation bandwidth is thus limited to about a gigahertz or so due to capacitance effects. On the other hand, in the case of travelling wave electrode geometry the bandwidth is given by

$$\Delta f_{3\text{dB}} = 1{\cdot}4c/\{[|N_0 - N_m|]\, L\},$$

where N_0 and N_m are the effective indices for optical and microwave frequencies. Thus the difference in velocity between the modulating microwave signal and the optical carrier limits the bandwidth and is about 6–7 GHz in the case of $LiNbO_3$.

4.4b *Intensity modulator.* Intensity modulation of light can be readily achieved by suitably combining phase modulation with a splitter/combiner. A waveguide interferometer of the Mach–Zehnder type which may be used as intensity modulator is constructed by combining two Y branches and straight-section phase modulators as shown in figure 6a.

As in the case of a phase modulator, a phase shift can be introduced by electrooptic control here also. In an interferometer the two arms of the straight portions can be driven by opposite polarity voltages thus achieving a push–pull configuration which gives twice the phase shift as compared to a single-phase modulator. This reduces the required voltage for a given phase shift.

In an interferometer the power is divided by the input Y-branch and is recombined

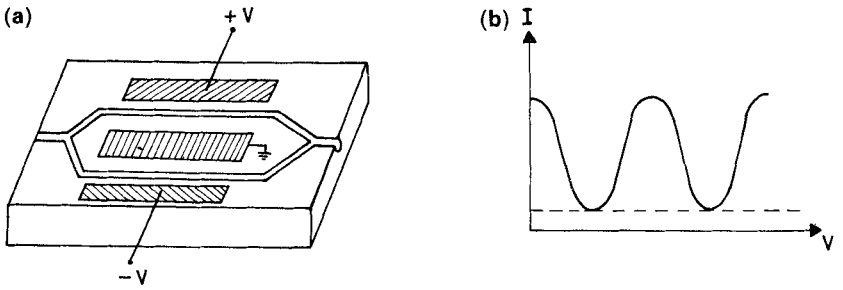

Figure 6. Schematic of (**a**) Mach–Zehnder interferometer and (**b**) its response.

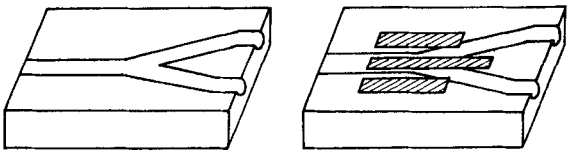

Figure 7. (**a**) Y-branch and (**b**) Y-branch switch.

after passing through the phase shifting segments by the output Y-branch. Assuming that there is no loss in the splitting and combining operations, the output is a superposition of the two guided modes arriving through the two arms and results in constructive and destructive interference. The transmission curve as a function of modulating voltage is shown in figure 6b. Normally for Z-cut $LiNbO_3$ only the TM mode is modulated efficiently. However the modulator can be made polarization independent by incorporating two sets of electrodes to control the TE and TM modes independently as shown by Burns *et al* (1978).

4.5 *Integrated optic Y-branch*

The Y-branch (figure 7) is usually a passive splitter/combiner though it can be made an active control device using the electrooptic effect. It can behave either as a mode converter/filter or as a power divider.

The modes incident on an asymmetric planar-dielectric branching waveguide with a shallow taper propagate such that the mode power is transferred to one arm of the branch or to the other. The principle is that a mode would choose the arm in which it could propagate with an effective index closest to the effective index that characterised its propagation before the waveguide divided. An asymmetric branching waveguide can thus be considered to act as a mode splitter. Symmetry considerations point out that in extreme cases of steep tapers or near symmetric branches, the branching waveguide will act, not as a mode splitter but as a power divider. In this case incident power concentrated in the upper part of the structure will end up in the upper arm and incident power concentrated in the lower part of the structure will end up in the lower arm independent of modal evolution.

The most important criteria for design of a Y-branch are the branching angle α, and width of the waveguides, W.

The angle α determines the mode separating and recombining functions as well as scattering losses in fork regions. It also determines how long the branching section (fork) has to be before the coupling between two arms is negligibly small and in turn determines the overall length of the device.

For a given mode propagation constant (β) of the planar guiding region, we have to decide on W to restrict the number of lateral modes to the required number.

The width of the straight-guide section and branching sections must be such that they are only single mode structures (i.e. one mode each in lateral and depth directions). For design details of Y-branch see Frenette & Cartledge (1988).

4.6 *Directional coupler switch*

A directional coupler (figure 8) consists of two waveguides in close proximity (parallel to each other) so that the evanescent field of one waveguide penetrates and couples into the latter waveguide's propagating mode. This is a sort of optical tunnelling to transfer

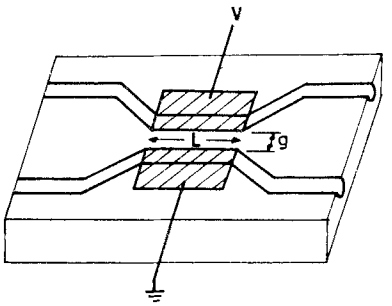

Figure 8. Directional coupler switch.

energy between the two structures. Energy transfer occurs after a certain length along the waveguide and the length at which maximum coupling occurs is called coupling length (L_c). Coupling length is a function of the structure and refractive index of the constituent waveguides and the intervening isolation region. Normally there will also be an input and an output section to enable the coupling of external fibres etc. An appropriate electrode pattern is also printed on to/adjacent to the guiding region to enable electrooptic control of light. The directional coupler (DC) can be used as intensity modulator, switch or in other ways.

The directional coupler switch design can be done in three stages: waveguide design, coupling length design and electrode design.

Waveguide design: The prime requisite here is that the refractive index of the guiding region must be greater than the index of the surrounding region. Though a lot of methods do exist to evaluate the boundary value problem for rectangular waveguides, we have used a method suggested by Sharma *et al* (1985). It uses a scalar variational principle with a cosine-exponential trial-field due to its simplicity and proven accuracy over the other methods.

Consider a waveguide having the following parameters as shown in figure 9a. Here,

n_s = refractive index of substrate (i.e. $LiNbO_3$) = 2·1398;
n_c = refractive index of cover (i.e. air) = 1;

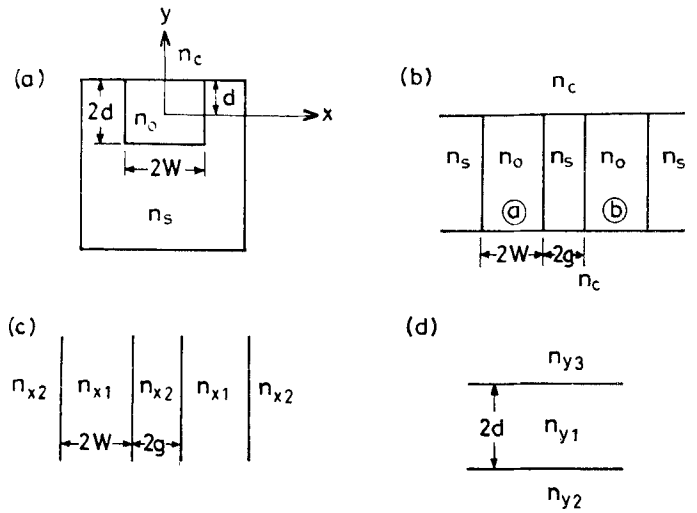

Figure 9. Design of a directional coupler using effective index method.

n_0 = refractive index of waveguide (i.e. Ti in $LiNbO_3$); $n_0 > n_s$;
$2d$ = depth of waveguide;
$2w$ = width of waveguide.

In a practical design reported earlier (Selvarajan *et al* 1988), $d/w = 0{\cdot}5$ and normalised frequency, $v_c = 0{\cdot}8\pi$ (for the fundamental mode) are used.

The refractive index distribution is assumed to be:

$$\begin{aligned} n^2(x,y) &= n_c^2; \quad y > d, \text{ all } x, \\ &= n_0^2; \ |y| < d, \ |x| < w, \\ &= n_s^2; \ |y| < d, |x| > w, \\ &= n_s^2; \quad y < -d, \text{ all } x. \end{aligned}$$

Now,

$$n_0 = n_s + \Delta n,$$

where Δn = change in refractive index due to titanium in-diffusion.

The value of Δn can be fixed as follows,

(1) v, Δn, and w are related by the equation $v = (2\pi w/\lambda)(n_0^2 - n_s^2)^{1/2}$ where, λ = wavelength of light in free space = $1{\cdot}32\,\mu$m, v = normalised frequency.
(2) Δn can change in steps of 1×10^{-3} from 2·1398 to 2·1498 so as to be practically realisable.
(3) For these values of Δn, the values of w are obtained for various values of v.
(4) A graph of w vs Δn is plotted for various v's. From this graph a suitable choice can be made for Δn and w.
(5) We choose an optimal value of $\Delta n = 5 \times 10^{-3}$ and the corresponding value of w is fixed at $3\,\mu$m for a v of 83% below cut-off, i.e. $\Delta n = 5 \times 10^{-3}$.

$$\begin{aligned} w &= 3\,\mu\text{m} \ (2w = \text{actual width} = 6\,\mu\text{m}), \\ v &= 0{\cdot}83 \times 0{\cdot}8 \times \pi, \\ d &= 1{\cdot}5\,\mu\text{m} \ (2d = \text{actual depth} = 3\,\mu\text{m}), \\ n_0 &= n_s + \Delta n = 2{\cdot}1398 + 5 \times 10^{-3} = 2{\cdot}1448. \end{aligned}$$

A suitable model for the scalar mode is obtained by assuming a model field distribution of apt form involving adjustable parameters and using this field in the variational analysis for the propagation constant, β.

Coupling length design: Since the mode fields of slab waveguides are well known, we adopt the same for ease of coupler design. The cross-sections and index distribution are as in figure 9b.

The refractive index distribution of equivalent slab coupling is given by (figures 9c & d),

$$\begin{aligned} n^2(x) &= n_{x1}^2; \quad g < |x| < 2w + g, \\ &= n_{x2}^2; \quad |x| < g, \\ &= n_{x2}^2; \quad |x| > 2w + g, \end{aligned}$$

where, $2g$ = inter-waveguide gap.

Hence, the problem of coupling between two rectangular waveguides reduces to determining the coupling between two slab waveguides. The coupling length, L_c, is given by

$$\frac{L_c}{\beta W^2} = \frac{[1 + p\tan(p)]}{2p^2 \sin^2 p} \exp[p\tan(p)\{2g/w\}],$$

substituting appropriate values ($p = 0{\cdot}4890$, $w = 3\,\mu$m and $g = 1\,\mu$m), $\beta = 10{\cdot}19313$, the coupling length is obtained as $L_c = 4{\cdot}48676$ mm.

Electrode design: The flow of optical power is controlled by placing an electrode and application of a voltage. The power transfer relation in the DC is as below:

$$P_a(z) = P_0 k^2 \cdot \sin^2[(k^2 + \delta^2)^{0{\cdot}5} \cdot L_c]/(k^2 + \delta^2),$$

where, $P_a(z)$ = power in waveguide (a), P_0 = power launched into one of the waveguides, δ = mismatch factor i.e. $\beta_a - \beta_b$, k = coupling coefficient.

When no voltage is applied,

$$\delta = 0; \quad P_a = P_0 \text{ and } (k^2 + \delta^2)^{0{\cdot}5} \cdot L_c = \pi/2,$$

i.e.

$$kL_c = \pi/2; \quad \text{for } L_c = 4{\cdot}5\,\text{mm}, \quad k = 0{\cdot}35/\text{mm}.$$

The switch is now said to be in the cross state.

When the applied voltage is V, the symmetry and hence the evanescent coupling is spoilt, and in this case no power transfer occurs

$$(k^2 + \delta^2)^{0{\cdot}5} \cdot L_c = \pi.$$

Hence,

$$\delta = \sqrt{3}\pi/(2L_c).$$

The switch is now said to be in the bar state.

An expression for the electrooptically induced phase shift is already given. From this we get

$$V/d = \sqrt{3} \cdot \lambda/(2L_c r_{33} n_0^3 \Gamma).$$

Substituting the values, $\lambda = 1{\cdot}32\,\mu$m, $L_c = 4{\cdot}487$ mm, $\Gamma = 0{\cdot}6$, $r_{33} = 31 \times 10^{-12}$ m/V and $n_0 = 2{\cdot}1448$; we get,

$$V/d = 1{\cdot}3880\,\text{V}/\mu\text{m}.$$

If we take $d = 3\,\mu$m, the required voltage $V = 4{\cdot}164$ volts.

Therefore the two electrodes can be placed with a gap of $3\,\mu$m and with an offset of $0{\cdot}5\,\mu$m with respect to the waveguide edge.

4.7 *Nonlinear integrated optic devices*

The area of nonlinear integrated optical devices came into being in 1982 when it was realized that standard integrated optic devices could be operated in an all-optical mode by introducing waveguide media with intensity dependent refractive indices. It is

believed that nonlinear integrated optical devices can be used for all optical signal processing at speeds limited only by the turn-off time of the nonlinearity which in the current state of art is of the order of subpicoseconds. A number of all-optical devices have already been reported. More of the device design and analysis than the actual realization of devices is in progress at present. To fabricate nonlinear guided wave devices, it is first necessary to fabricate waveguides out of nonlinear materials and to characterize their nonlinear properties. Material requirements for nonlinear devices are very different from those of linear integrated optic devices.

$LiNbO_3$ is one of the bulk nonlinear materials useful in integrated optics. Another class of materials which is of intense research interest is semiconductor-doped glasses. Waveguides have been made on these glasses by ion exchange in a fashion similar to that used in the fabrication of waveguides in ordinary sodium glass for linear optics. Multiple quantum wells in semiconductors is another area of intense interest. Yet another area of interest for nonlinear integrated optics is that of monomers and multilayers of monomers of organic materials formed by the Langmuir–Blodgett technique. Most of these materials and the associated techniques are in the experimental stage and can be expected to become practical soon.

All optical functions such as switching, logic, limiting, thresholding and modulation have been predicted for use in nonlinear integrated optic form. These include nonlinear directional coupler, nonlinear grating devices, nonlinear mode sorters, nonlinear Mach–Zehnder interferometer and nonlinear optical bistable devices (Assanto 1990).

5. Applications

5.1 *Photonic switching*

Photonic switching is being envisaged as one of the more promising answers to requirements of high data-rates and reliability posed by future optical systems. In this context, optical switching network architectures such as space division (SD), time division (TD) and wavelength division (WD) have been studied for future systems. The need to develop and establish photonic switching is driven by the demand for system bandwidth – upto the point where the bit rates are high enough to impose severe demands on the electronic parts of the system. When switching times required are below the order of 10^{-11} seconds, it becomes obvious that photonics is the only available technology. In the region of $10^{-11} - 10^{-5}$ seconds, where the bandwidth of the signal is to be preserved, integrated optic devices are often used, using electrical control, to route light from one single-mode waveguide to another. The popularity of parallel computing environments provides yet another impetus to the development of connecting networks made of arrays of switches, which were termed multistage interconnection networks (MIN). With the growing awareness that optical computing is the next logical step in the development of computing, and of the scarcity of media which could reliably carry and switch the signals that these new computing systems would require, photonic switching emerges as the technology of both choice and necessity.

Due to the development of integrated optics, a host of basic integrated optic photonic switching elements (IOBPSE) are available today. A recent review of IOBPSE on $LiNbO_3$ can be referred to for more details (Selvarajan & Midwinter 1989). Novel switches and new concepts continue to be reported, combining a high switching

efficiency with a low substrate area utilization. A new family of architectures termed the SSPIRAL has been proposed for realisation as planar photonic switching MIN by Subrat Kar & Selvarajan (1990).

Attenuation, insertion loss, differential insertion loss, device insertion loss, crosstalk, waveguide insertion loss, extinction ratio, coupling loss, polarization insensitivity, channel-rate transparency and the signal-to-crosstalk ratio are figures of merit which characterize any photonic switch array.

Due to the high length–width ratio of the IOBPSE, integration is limited to a few tens of devices considering the size constraints of substrate crystals (upto 16 × 16 on a single substrate are known). For large sizes, interconnected substrates containing smaller arrays can be considered.

5.2 *Optical computing*

Optical computing is an emerging field and has generated considerable excitement all around. Many theoretical aspects of optical computing such as architectures, interconnection topologies and routing and other algorithms are rapidly advancing. It all started with generally borrowed concepts from electronic digital and analog computing. However, new concepts unique to photonics, such as highly parallel architectures, are now evolving. On the implementation side, bulk optics is being largely used. Since integrated optics in itself is a developing technology it may be a while before it penetrates the computing field. An integrated optic matrix–matrix multiplier was reported by Tsai (1988). In this case electrooptic Bragg modulator array, microlenses and channel waveguides are suitably integrated on to a Y-cut $LiNbO_3$ crystal. A practical device to implement 2 × 2 matrix–matrix multiplication showed a dynamic range of 31 dB. A variety of other developments including chip-to-chip optical interconnections, array processing and semiconductor devices for optical computing have been reported (Ishihara 1990).

5.3 *RF spectrum analysis*

Real-time spectral analysis of wideband RF signals is required in many cases like electronic warfare, radar signal processing, radio astronomy and laser-based measuring systems. Conventional spectrum analysers have both speed and bandwidth limitations in addition to being bulky. Integrated optic solutions are attractive as they are capable of overcoming the above limitations. There are three possible structures: monolithic, quasi-monolithic and hybrid structures. In the monolithic case, the structure is expected to fully integrate all the components like the source, waveguide devices, detector arrays and electronic circuits; in quasi-monolithic, a partial integration is expected. Both these attempts need the semiconductor technology. While these are the ultimate objectives presently there is no IO spectrum analyser which is monolithic. In the hybrid approach the source and detector array are chip-bonded to an IO analyser (usually $LiNbO_3$). Many versions of this type are reported in the literature. They include the use of geodesic, Luneberg or Fresnel lenses, folded type structure, use of silicon technology, acoustooptic or electrooptic grating fields and so on.

An early version of the IO spectrum analyser is described by Barnoski *et al* (1979). An injection laser diode and a linear detector array with CCD read-out are chip-bonded to an $LiNbO_3$ IO device comprising Ti diffused planar waveguide, two geodesic lenses and

surface acoustic wave transducers. Dynamic range of 41 dB, channel isolation of 28 dB and a channel resolution of 4 MHz over a 400 MHz bandwidth have been reported.

6. Conclusion

It is evident from the foregoing presentation that integrated optics has emerged as a practical means to achieve compact lightwave systems. Due to space limitations the technology and applications of IO could not be dealt with in detail in this article. For further reading, the reader is referred to the special issue of the *Proceedings of the IEEE* (November 1987) and books by Nishihara *et al* (1987) and Hutcheson (1987).

References

Alferness C 1982 Waveguide electrooptic modulators. *IEEE Trans. Microwave Theory Tech.* 30: 1121–1137

Assanto G 1990 All optical nonlinear integrated devices. *J. Mod. Opt.* 37: 855–873

Barnoski M K, Chen B, Joseph T R, Lee J Y, Ramer O G 1979 Integrated optic spectrum analyser. *IEEE Trans. Circuits Syst.* 26: 1113–1124

Brabander G N, Boyd J T, Jackson H E 1991 Single polarization optical waveguide on silicon. *IEEE J. Quantum Electron.* 27: 575–579

Burns W K, Giallorenzi T G, Moeller R P, West E J 1978 Interferometric waveguide modulator with polarization independent operation. *Appl. Phys. Lett.* 33: 944–947

Burns W K, Klein P H, West J, Plow L E 1979 Ti diffusion in Ti: $LiNbO_3$ planar and channel optical waveguides. *J. Appl. Phys.* 50: 6175–6182

Deri R J, Kapon E 1991 Low loss III–V semiconductor optical waveguides. *IEEE J. Quantum Electron.* 27: 626–640

Findalky T, Chen B 1984 Single mode transmission selective integrated optical polarizers in $LiNbO_3$. *Electron. Lett.* 20: 128–129

Frenette N J P, Cartledge J C 1988 Using longitudinal variations in branching angle to optimise power division or mode splitting properties of planar Y branch waveguides. *IEEE J. Quantum Electron.* 4: 2491–2499

Ghatak A K, Thyagarajan K 1989 in *Optical electronics* (Cambridge: University Press) chap. 14

Honkanen S, Tervonen A 1988 Experimental analysis of $Ag^+ - Na^+$ exchange in glass with silver film ion sources for planar waveguide techniques. *J. Appl. Phys.* 63: 634–639

Hutcheson L D (ed.) 1987 *Integrated optical circuits and components: Design and applications* (New York: Marcel Dekker)

Ishihara S (ed.) 1990 *Optical computing in Japan* (Tokyo: Nova Science)

Kogelnik H 1975 in *Integrated optics* (ed.) T Tamir (Berlin: Springer–Verlag) chap. 2

Loni A, Hay G, De La Rue R M, Winfield J M 1989 Proton exchanged $LiNbO_3$ waveguides. *J. Lightwave Technol.* 7: 911–919

Miller S E 1969 Integrated optics: an introduction. *Bell Syst. Tech. J.* 48: 2059–2068

Nishihara H, Haruna M, Suhara T 1987 *Optical integrated circuits* (New York: McGraw-Hill)

Ramaswamy R V and Srivastava R 1988 Ion exchanged glass waveguides. *J. Lightwave Technol.* 6: 984–1002

Satyanarayana M V, Srinivas T, Selvarajan A 1992 Electrostatic field analysis of electrooptic devices. *J. Electromag. Waves Appl.* 6: 143–155

Selvarajan A 1986 Computer simulation and experimental studies on fibre optic boradcase system, Project report, IISc–ISRO/STC/15 K, Indian Institute of Science, Bangalore

Selvarajan A, Midwinter J E 1989 Photonic switches and switch arrays on $LiNbO_3$. *Opt. Quantum Electron.* 21: 1–15

Selvarajan A, Shankar J, Krishna T R 1988 Design of a 4 × 4 switch and a phase modulator, Technical Report, ITI–IISc Project on photonic circuits, Indian Institute of Science, Bangalore

Shani Y, Henry C H, Kistler R C, Kazaniniv R F, Orlowsky K J 1991 Integrated optic adiabatic devices on silicon. *IEEE J. Quantum Electron.* 27: 556–566

Sharma A, Misra P K, Ghatak A K 1988 Single mode optical waveguides and directional couplers with rectangular cross section: A simple and accurate method of analysis. *J. Lightwave Technol.* 6: 1119–1125

Shiva Kumar, Srinivas T, Selvarajan A 1990 Beam propagation method and its applications to integrated optic structures and optical fibres. *Pramana – J. Phys.* 34: 347–358

Subrat Kar, Selvarajan A 1990 Some novel photonic guided-wave space-switching architectures. *J. Inst. Electron. Telecommun. Eng.* 36: 513–519

Takahashi H, Ohmori Y, Kawachi M 1991 Design and fabrication of silica based integrated optic 1 × 128 power splitter. *Electron. Lett.* 27: 2131–2132

Takato N, Jingaji K, Yasu M, Toba H, Kawachi M 1988 Silica based single mode waveguides on silicon and their application to guided wave optical interferometers. *J. Lightwave Technol.* 6: 1003–1010

Takono T, Hamasaki J 1972 Propagating modes of a metal clad dielectric slab waveguide for integrated optics. *IEEE J. Quantum Electron.* 8: 206–212

Tsai C S 1988 Integrated optical device modules in $LiNbO_3$ for computing and signal processing. *J. Mod. Opt.* 33: 965–977

Van Tomme E, Van Daele P P, Baets R G, Lagasse P E 1991 Integrated optic devices based on nonlinear optical polymers. *IEEE J. Quantum Electron.* 27: 778–787

Zang D Y, Tsai C S 1985 Single mode WG microlens and microlens array fabrication in $LiNbO_3$ using TIPE technique. *Appl. Phys. Lett.* 46: 703–705